

Preparation, characterization and conductivity studies of $\text{Li}_{3-2x}\text{Al}_{2-x}\text{Sb}_x(\text{PO}_4)_3$

N ANANTHARAMULU, G PRASAD[†] and M VITHAL*

Department of Chemistry, [†]Department of Physics, Osmania University, Hyderabad 500 007, India

MS received 10 October 2007; revised 27 December 2007

Abstract. New NASICON type materials of composition, $\text{Li}_{3-2x}\text{Al}_{2-x}\text{Sb}_x(\text{PO}_4)_3$ ($x = 0.6$ to 1.4), have been prepared and characterized by powder XRD and IR. D.C. conductivities were measured in the temperature range 300–573 K by a two-probe method. Impedance studies were carried out in the frequency region 10^2 – 10^6 Hz as a function of temperature (300–573 K). An Arrhenius behaviour is observed for all compositions by d.c. conductivity and the Cole–Cole plots obtained from impedance data do not show any spikes on the lower frequency side indicating negligible electrode effects. A maximum conductivity of 4.5×10^{-6} S cm^{-1} at 573 K was obtained for $x = 0.8$ of the $\text{Li}_{3-2x}\text{Al}_{2-x}\text{Sb}_x(\text{PO}_4)_3$ system.

Keywords. NASICON; X-ray diffraction; infrared spectra; impedance.

1. Introduction

Skeletal materials based on sodium zirconium silico phosphate ($\text{Na}_{1+x}\text{Zr}_2\text{P}_{3-x}\text{Si}_x\text{O}_{12}$, $0 \leq x \leq 3$), popularly known as NASICON and sodium zirconium phosphate ($\text{NaZr}_2\text{P}_3\text{O}_{12}$) abbreviated as NZP, have attracted considerable attention during the last 25 years and are investigated by several groups (Hong 1976). The reasons for such an explosive growth of investigations are not far to seek. The crystal chemistry of such materials is unique and possesses a framework structure with fast Na^+ transport comparable to that of β' -alumina (Hong 1976; Goodenough *et al* 1976). The framework structure is a rigid, three-dimensional network of PO_4 (or SiO_4) tetrahedra sharing corners with ZrO_6 octahedra encapsulating the mobile sodium ion in the interconnected interstitial space. It is observed that majority of materials belonging to NASICON or NZP type crystallizes in the hexagonal lattice while a few of them adopt monoclinic lattice. These materials are abbreviated as $\text{AMM}'\text{P}_3\text{O}_{12}$, where site 'A' can be occupied by alkali, alkaline earth ions, Cu^{2+} , Cu^+ , Ag^+ , H^+ , H_3O^+ , NH_4^+ , while M and M' can be filled with transition metal ions. Phosphorous can be partially substituted by silicon. Thus the structure is flexible for substitution at A, M, M' and P sites, giving rise to a large number of isostructural compounds. The potential applications of NASICON type materials are well documented (Roy *et al* 1982; Agrawal and Adair 1990; Gopalakrishnan and Kasturi Rangan 1992; Hirose and Kuwano 1994; Govindan Kutty *et al* 1998; Meunier *et al* 1998; Balagopal *et al* 1999; Lightfoot *et al*

1999; Brik *et al* 2001; Pasciak *et al* 2001; Wang and Kumar 2003). At present, there is an intense interest in finding a lithium ion conductor with high conductivity and other properties suitable for utilization in high energy density batteries and other electrochemical devices (Irvine and West 1989). The low equivalent weight and the high electropositive nature of Li which gives high cell voltage and high density of advanced electrochemical devices, paved the way for an intense search for a good ionic conductor with the requisite ceramic properties over the past several years. Goodenough *et al* designed new cathode materials for rechargeable lithium batteries with NASICON structure of compositions, $\text{Li}_3\text{Fe}_2(\text{XO}_4)_3$ ($\text{X} = \text{P}, \text{As}$) and $\text{Li}_2\text{NaV}_2(\text{PO}_4)_3$ (Masquelier *et al* 1998; Cushing Brian and Goodenough 2001). The crystal structures of several materials of composition, $\text{AM}^{\text{III}}\text{M}^{\text{V}}(\text{PO}_4)_3$ ($\text{A} = \text{Li}$ or Na), have been reported (Rangan and Gopalakrishnan 1995; Rivier *et al* 1995). However, the electrical properties have not been reported for many of these materials. It is observed that a high lithium ion conductivity of above 10^{-4} S cm^{-1} was shown by the solid solutions, $\text{Li}_{1+x}\text{Ti}_{2-x}\text{M}(\text{III})_x(\text{PO}_4)_3$ ($\text{M} = \text{Al}, \text{Sc}, \text{In}$, etc) and the phase transition does not influence the conductivity of $\text{Li}_3\text{M}_2(\text{PO}_4)_3$ ($\text{M} = \text{Cr}, \text{Sc}, \text{In}$) based systems (Subramanian *et al* 1986; Lin *et al* 1988; Aono *et al* 1990, 2004; Nagganovsky and Sigaryov 1992). Recently, for $\text{Li}_{3-2x}\text{Cr}_{2-x}\text{Ta}_x(\text{PO}_4)_3$ system, the maximum conductivity of 8.4×10^{-6} S cm^{-1} at 298 K for $x = 0.8$ was obtained and it has been enhanced by about three to five times by the addition of lithium salts like Li_2O or Li_3PO_4 or Li_3BO_3 (Aono *et al* 2004). In continuation of our work on NASICON related materials, specially Li and Sb containing compositions (Rambabu *et al* 2006), we report here the preparation, characterization

*Author for correspondence (muga_vithal@osmania.ac.in)

and conductivity studies of NASICON type solid solution of composition, $\text{Li}_{3-2x}\text{Al}_{2-x}\text{Sb}_x(\text{PO}_4)_3$ ($x = 0.6-1.4$) (hereafter abbreviated as $\text{LASP}(x)$).

2. Experimental

The solid solutions of $\text{LASP}(x)$ were prepared by sequential heating of stoichiometric mixtures of Li_2CO_3 , Sb_2O_5 , Al_2O_3 and $\text{NH}_4\text{H}_2\text{PO}_4$ (all AR grade chemicals) at 500°C (5 h), 700°C (5 h) and finally at 800°C (20 h) in air with intermediate grindings. Attempts to prepare compositions with $x < 0.6$ either resulted in the melt formation or mixture of unknown phases. Heating the reactants at a lower temperature ($< 800^\circ\text{C}$) for very long periods was also not successful. Thus the phase formation range in the present $\text{LASP}(x)$ series was $0.6 \leq x \leq 1.4$ under the present experimental conditions. Powder X-ray diffractograms were recorded using Philips Expert Analytical X-ray diffractometer. Nickel filtered Cu-K_α radiation of wavelength, 1.5406 \AA , was used. XRD patterns were indexed and lattice parameters were calculated from the d -spacing of the powder pattern using a least squares minimization program 'POWD' developed by Wu (1989). Experimental densities were measured by Archimedes' principle using xylene as an immersion liquid. Calculated densities were obtained from lattice parameters. Infrared spectra were recorded in the form of KBr pellets using JASCO FT/IR-5300 Spectrometer. The d.c. conductivities in the temperature range $300-573 \text{ K}$ were measured using a two-

probe method on the sintered pellets coated with silver paint. For this a conventional sample holder and Keithley Electrometer 610C were used. A.C. impedance measurements were carried out by using HP4192a impedance analyser. The temperature range of impedance measurements was $300-573 \text{ K}$ and the frequency range, $100 \text{ Hz}-1 \text{ MHz}$.

3. Results and discussion

3.1 Powder XRD

The powder XRD patterns of $\text{LASP}(x)$ are shown in figure 1. All the compositions (except for $x = 0.6$ and 0.8) are found to be single phase with no detectable impurities or unreacted starting materials. The d -lines observed for $x = 1.4$, 1.2 and 1 compositions (i.e. for $\text{Li}_{0.2}\text{Al}_{0.6}\text{Sb}_{1.4}(\text{PO}_4)_3$, $\text{Li}_{0.6}\text{Al}_{0.8}\text{Sb}_{1.2}(\text{PO}_4)_3$ and $\text{LiAlSb}(\text{PO}_4)_3$) clearly suggest a hexagonal lattice for these phases. For $x = 0.8$ and 0.6 compositions (i.e. for $\text{Li}_{1.4}\text{Al}_{1.2}\text{Sb}_{0.8}(\text{PO}_4)_3$ and $\text{Li}_{1.8}\text{Al}_{1.4}\text{Sb}_{0.6}(\text{PO}_4)_3$), though majority of observed d -lines correspond to hexagonal NASICON phase, d -lines belonging to monoclinic NASICON phase are noticed. For instance, the two d -lines in the range $2\theta \approx 13-17^\circ$ corresponding to 020 and 111 planes, respectively belong to monoclinic NASICON phase (Aono *et al* 2004). These two compositions cannot be regarded as pure monoclinic phase due to the following observations: (i) observation of intense peaks at $2\theta \approx 21, 22, 25, 31$ and 34° which are

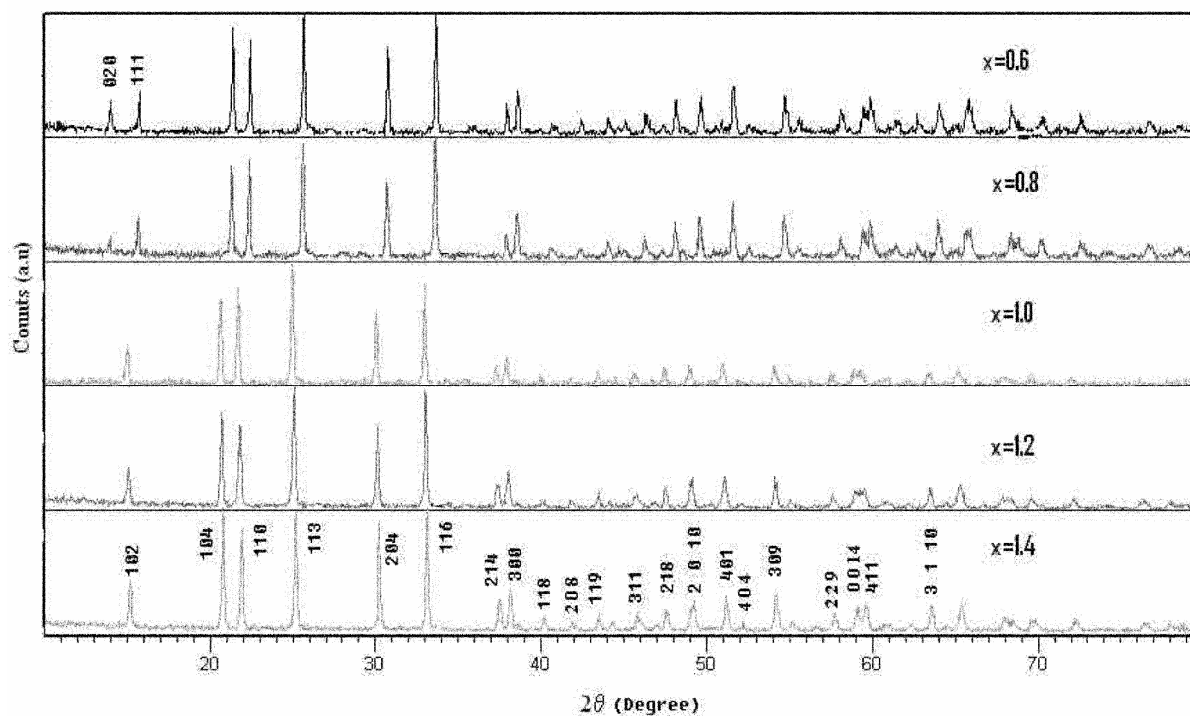


Figure 1. Powder X-ray diffractograms of $\text{LASP}(x)$.

Table 1. Composition, lattice parameters and densities of LASP(x).

Composition	Lattice parameters		Density		Reference
	$a(\text{\AA})$	$c(\text{\AA})$	$d_{\text{obs}}(\text{g cm}^{-3})$	$d_{\text{cal}}(\text{g cm}^{-3})$	
LASP ($x = 0.6$)	8.282	21.708	3.10	3.15	Present work
LASP ($x = 0.8$)	8.261	21.866	3.26	3.27	Present work
LASP ($x = 1.0$)	8.306	22.557	3.21	3.26	Present work
LASP ($x = 1.2$)	8.303	21.470	3.50	3.55	Present work
LASP ($x = 1.4$)	8.301	21.629	3.61	3.65	Present work
$\text{LiSbFeP}_3\text{O}_{12}$	8.44	21.48	3.52	3.55	Rambabu <i>et al</i> (2006)
$\text{LiSbCrP}_3\text{O}_{12}$	8.24	21.13	3.48	3.52	Rambabu <i>et al</i> (2006)
$\text{AgTaAlP}_3\text{O}_{12}$	8.44	22.10	4.09	4.39	Koteswara Rao <i>et al</i> (2005)
$\text{AgTaGaP}_3\text{O}_{12}$	8.41	21.90	4.66	4.77	Koteswara Rao <i>et al</i> (2005)
$\text{AgTaFeP}_3\text{O}_{12}$	8.40	21.90	4.35	4.68	Koteswara Rao <i>et al</i> (2005)

Table 2. Powder X-ray diffraction data for LASP ($x = 0.8$).

hkl	$d_{\text{obs}}(\text{\AA})$	$d_{\text{cal}}(\text{\AA})$	I_{obs}	I_{cal}
1 0 2	5.9766	5.9865	276	290
1 0 4	4.3325	4.3437	632	640
1 1 0	4.1306	4.1305	307	312
1 1 3	3.5914	3.5936	980	1000
2 0 4	2.9920	2.9932	286	284
1 1 6	2.7298	2.7328	470	467
2 1 4	2.4238	2.4238	77	76
3 0 0	2.3870	2.3848	93	89
3 0 6	1.9959	1.9955	13	12
2 1 8	1.9211	1.9223	124	120
2 0 10	1.8655	1.8657	69	67
3 0 8	1.7977	1.7970	56	55
4 0 4	1.6999	1.6999	10	10
2 2 9	1.5736	1.5736	54	54
0 0 14	1.5627	1.5619	60	61
3 1 10	1.4695	1.4694	156	155

due to hexagonal NASICON phase and (ii) absence of low intense d lines at $2\theta \approx 22\text{--}24^\circ$ and $26\text{--}30^\circ$ corresponding to monoclinic phase. Thus the compositions, $\text{Li}_{1.4}\text{Al}_{1.2}\text{Sb}_{0.8}(\text{PO}_4)_3$ and $\text{Li}_{1.8}\text{Al}_{1.4}\text{Sb}_{0.6}(\text{PO}_4)_3$, can be regarded as predominantly hexagonal with a trace of monoclinic phase. It is expected that for $x < 0.6$ compositions the monoclinic phase may be formed with or without trace of hexagonal phase. Similar results were obtained for $\text{Li}_{3-2x}\text{Cr}_{2-x}\text{Ta}_x(\text{PO}_4)_3$ system (Aono *et al* 2004). The lattice parameters for all the compositions are derived assuming hexagonal lattice. The lattice parameters thus obtained are presented in table 1 with the calculated and observed densities for all the compositions along with other similar compositions for comparison. The observed and calculated d -spacing and intensities of various hkl reflections for $\text{Li}_{1.4}\text{Al}_{1.2}\text{Sb}_{0.8}(\text{PO}_4)_3$ are presented in table 2.

3.2 IR spectra

The IR spectra of LASP(x) compositions are recorded in the range $2000\text{--}400\text{ cm}^{-1}$. All the compositions exhibit

strong absorptions below 1500 cm^{-1} and the assignments of the bands are presented in table 3. Generally the vibrational modes of NASICON phases can be assigned to PO_4 tetrahedra (internal and external modes) and to lattice modes of metal octahedra. Of these, the bands corresponding to PO_4 unit are intense than metal octahedral bands. The assignments for the observed bands have been made based on the predictions of factor group analysis (Nakamoto 1978; Barj *et al* 1983; Mbandza *et al* 1985). The PO_4 unit gives nine vibrational modes that are characterized by non-degenerate symmetric $\nu_s(\text{PO})$ (ν_1), antisymmetric triply degenerate $\nu_a(\text{PO})$ (ν_3) of phosphorous non-bridging oxygen stretching and the symmetric doubly degenerate $\delta_a(\text{OPO})$ bending (ν_2) and antisymmetric triply degenerate $\delta_a(\text{OPO})$ bending (ν_4) (Mbandza *et al* 1985; Barj *et al* 1992). These modes are observed in the frequency ranges $1270\text{--}1000\text{ cm}^{-1}$ (ν_3), $1000\text{--}900\text{ cm}^{-1}$ (ν_1), $670\text{--}540\text{ cm}^{-1}$ (ν_4) and $450\text{--}440\text{ cm}^{-1}$ (ν_2) for all the compositions under investigation. The PO_4 external modes corresponding to vibrational and translational motions of these groups are generally observed below 300 cm^{-1} . Due to the instrumental constraints the spectra could not be recorded below 400 cm^{-1} and hence the corresponding assignments could not be made. The absence of any IR bands in the region $740\text{--}730\text{ cm}^{-1}$ proves the absence of pyro phosphate ($\text{P}_2\text{O}_7^{4-}$) impurity. Similar types of spectra are obtained for sodium and lithium analogues (Rangan and Gopalakrishnan 1995).

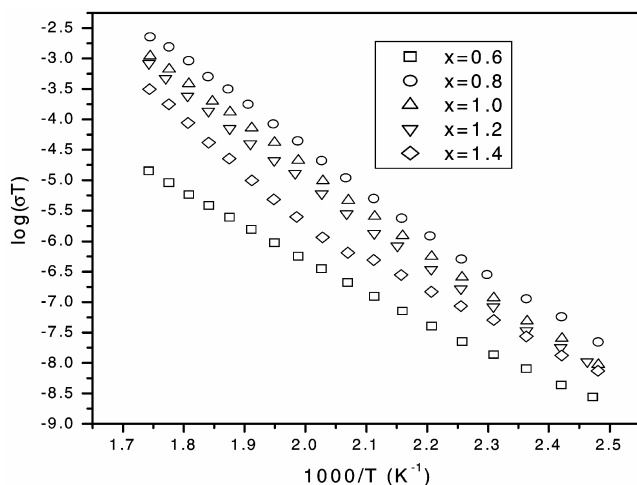
3.3 D.C. conductivity

The d.c. conductivity values are calculated from the bulk resistance and sample dimensions in the temperature range $300\text{--}573\text{ K}$. Figure 2 shows the variation of $\log(\sigma T)$ with $1000/T$ for all compositions and a linear relationship is obtained. A comparison between (i) the temperature dependence of conductivity and (ii) change in the structure with the value of x is worth mentioning. It is observed that in the system LASP(x), for $x \geq 1$, it crystallizes in hexagonal lattice while for $x < 1$ the monoclinic phase

Table 3. IR spectral data for LASP(*x*).

Composition	$\nu_3\nu_d$ (P–O)	$\nu_1\nu_s$ (P–O)	$\nu_4\delta_d$ (O–P–O)	$\nu_2\delta_d$ (O–P–O)
LASP (<i>x</i> = 0.6)	1206 w, 1179 w, 1136 s, 1084 w, 1038 w	989 vs	635 m, 607 s	419 vs
LASP (<i>x</i> = 0.8)	1208 sh, 1140 m, 1083 w, 1032 w	988 s	636 s, 603 m	420 vs
LASP (<i>x</i> = 1.0)	1210 sh, 1140 m, 1081 w, 1029 w	988 s	636 s, 603 m	419 vs
LASP (<i>x</i> = 1.2)	1225 m, 1126 m, 1028 m	953 sh	676 vs, 633 vs, 592 m, 547 m	–
LASP (<i>x</i> = 1.4)	1229 m, 1176 sh, 1108 sh, 1028 s	930 w	673 vs, 630 vs, 595 vs, 546 s	–

The band positions are in cm^{-1} ; vs = very sharp, s = sharp, m = medium, w = weak, b = broad and sh = shoulder.

**Figure 2.** Arrhenius plots of LASP(*x*).

starts crystallizing. It is reasonable to expect differences in the temperature dependence of conductivity in these phases. However, in the present investigation, the conductivity variation with temperature is similar for all the compositions i.e. for LASP(*x*). This indicates that the $\text{Li}_3\text{Al}_2(\text{PO}_4)_3$ based system does not have a change in conductivity associated with the structural phase transition as reported for $\text{Li}_3\text{Cr}_2(\text{PO}_4)_3$, $\text{Li}_3\text{In}_2(\text{PO}_4)_3$ and $\text{Li}_3\text{Sc}_2(\text{PO}_4)_3$ (Naggarovsky and Sigaryov 1992; Aono *et al* 2004). It is observed from the figure that the conductivity increases with increase in temperature. The behaviour of variation of conductivity with temperature is similar to that observed in other NASICON type of compounds. The data were fitted to Arrhenius equation

$$\sigma_{d.c.}T = \sigma_0 \exp(-E_\sigma/kT), \quad (1)$$

where σ_0 is the pre-exponential factor, T the absolute temperature, E_σ the activation energy for conduction and k the Boltzmann's constant. From the slopes of these straight lines, the activation energies (E_a d.c.) for conduction are calculated and fall in the range 1–1.4 eV (table 4).

3.4 Impedance studies

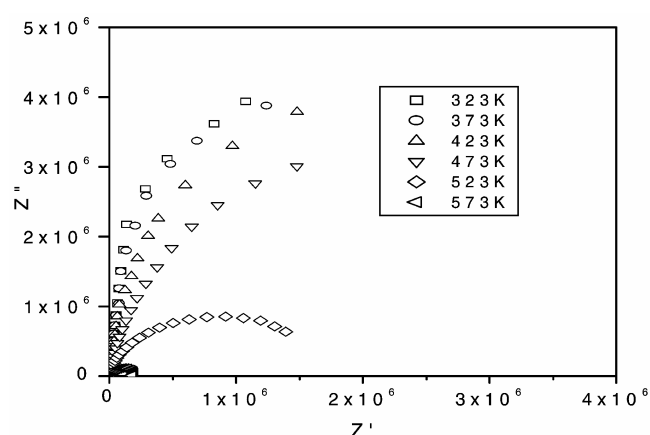
In the present paper, the impedance data of $x = 0.8$ is analysed in detail (similar impedance and modulus spectro-

scopy data were observed for all remaining compositions). The impedance data for LASP ($x = 0.8$) is represented in two different types of figures: (a) Cole–Cole plots of real (Z') and imaginary (Z'') parts of impedance (figure 3) and (b) frequency explicit plots of imaginary part of impedance (Jonscher 1980). All the frequency dependent graphs of Z'' show a peak in the temperature range 473–573 K. In those plots where peaks are observed, the peak frequency is found to be a function of temperature. The inverse of peak frequency as a function of temperature on a semi log scale is plotted as $\log \tau$ vs $1000/T$. The straight line behaviour of this graph indicates Debye like behaviour of dipoles responsible for the peak in Z'' vs frequency plots (Enrique Losilla *et al* 1998). The relaxation time of dipoles is found to decrease with increase in temperature. The calculated activation energy (E_a relax) for relaxation is 0.76 eV. The small activation energy for relaxation indicates the presence of associated charged defects. The complex impedance plots does not show semicircles up to 323 K but as the temperature increases the curves attain greater curvature and become perfect semicircles. All these plots terminate at the origin indicating the absence of series resistance in the equivalent circuit model of the sample. The absence of spike at the lower frequency side of Cole–Cole plots indicates negligible electrode effects. All the semicircles start on the real impedance axis at the lowest frequency. This starting point is found to decrease with increase in temperature. Low frequency intercepts of these semicircles on real axis give the resistance of the sample at the temperature of the Cole–Cole plots. The conductivity of all the samples is calculated from these intercepts and plotted as a function of inverse of temperature on semi log scale. The activation energy (E_a bulk) of conductivity from these plots is 0.77 eV for LASP ($x = 0.8$) composition. It is observed that E_a (bulk) is very close to activation energy for relaxation (E_a relax) for all the compositions (table 4).

The frequency variation of conductivity shows two slopes at all the temperatures of the present measurements. The low frequency and low temperature conductivity could be because of the intrinsic defects and charge agglomerations present in the sample. The variation of slope of conductivity plots at lower frequency is an indication of presence of such defects. These graphs can be fit to the equation (Elliott 1994)

Table 4. The d.c. conductivities of all compositions at 423 K and 573 K with activation energy of conduction (E_a d.c.). The $\sigma(0)$ (at 423 K) obtained by fitting the a.c. conductivity data to (2) and the activation energies for bulk conductivity and dielectric relaxation.

Composition	From d.c. conductivity		From a.c. impedance			
	$\sigma_{d.c.}$ at 423 K ($\text{ohm}^{-1} \text{cm}^{-1}$)	$\sigma_{d.c.}$ at 573 K ($\text{ohm}^{-1} \text{cm}^{-1}$)	E_a d.c. (eV)	$\sigma(0)$ at 423 K ($\text{ohm}^{-1} \text{cm}^{-1}$)	E_a (bulk) (eV)	E_a (relax) (eV)
LASP ($x = 0.6$)	1.9×10^{-11}	3.5×10^{-8}	1.01	1.8×10^{-11}	0.49	0.46
LASP ($x = 0.8$)	4.7×10^{-8}	4.5×10^{-6}	1.37	4.11×10^{-8}	0.77	0.76
LASP ($x = 1.0$)	8.8×10^{-9}	3.6×10^{-7}	1.37	6.3×10^{-9}	0.57	0.54
LASP ($x = 1.2$)	1.2×10^{-8}	3.6×10^{-6}	1.35	3.9×10^{-8}	0.67	0.63
LASP ($x = 1.4$)	1.3×10^{-11}	7.2×10^{-8}	1.22	1.4×10^{-11}	0.71	0.75

**Figure 3.** Complex impedance plots of LASP ($x = 0.8$).

$$\sigma(\omega) = \sigma_0 + A\omega^{n1} + B\omega^{n2}, \quad (2)$$

where A , B , $n1$ and $n2$ are constants.

The plots of imaginary parts of the impedance, Z'' and electric modulus, M'' , against log frequency show single peak in both Z'' and M'' spectra separated by less than half a decade of frequency. The peak width at half height is about 1.22 decades, which is close to 1.14 decades expected for Debye peak (Enrique Losilla *et al* 1998). Since Z'' and M'' peaks are almost coincident and there is no evidence of any additional peaks at lower frequencies in the Z'' spectrum, the observed results represent bulk conductivities. The absence of additional peaks in the Z'' spectrum indicates no grain boundary contributions to impedance and the observed results are due to bulk (grain) conductivity only.

4. Conclusions

New lithium NASICON of composition, $\text{Li}_{3-2x}\text{Al}_{2-x}\text{Sb}_x(\text{PO}_4)_3$ ($x = 0.6$ to 1.4), is prepared and characterized by IR and powder XRD. LASP(x) compositions in the range $1 \leq x \leq 1.4$ crystallize in hexagonal lattice of NASICON framework while for $0.6 \leq x < 1$ compositions a trace of monoclinic phase was observed. These samples show characteristic PO_4 vibrations. The activation energies

obtained from d.c. conductivities are in the range 1–1.4 eV. The activation energies obtained from (i) frequency explicit $\log(\omega)_{\max}$ vs inverse of temperature and (ii) Cole–Cole $\log f_{\max}$ vs inverse of temperature plots are of the same order. All the Cole–Cole plots terminate at the origin indicating the absence of series resistance in the equivalent circuit model of the sample. The presence of a single peak in the plots of both $\log f$ vs Z'' and $\log f$ vs M'' indicates bulk conductivity and absence of any grain boundary contribution to impedance. The height, full width at half maximum of the M''_{\max} peak and near coincidence of the M''_{\max} and Z''_{\max} peaks in these plots suggest the Debye behaviour of this sample.

Acknowledgements

The authors would like to thank Head, Department of Physics, Osmania University, Hyderabad, for providing powder XRD facility.

References

- Agrawal D K and Adair J H 1990 *J. Am. Chem. Soc.* **71** 2153
- Aono H, Sugimoto E, Sadaoka Y, Imanaka N and Adachi G 1990 *J. Electrochem. Soc.* **137** 1023
- Aono H, Muhammad Asri bin Idris and Yoshihiko Sadaoka 2004 *Solid State Ionics* **166** 53
- Balagopal S, Landro T, Zecevic S, Sutija D, Elangovan S and Khandkar A 1999 *Sep. Purif. Technol.* **15** 231
- Barj M, Perthuis H and Colombon Ph 1983 *Solid State Ionics* **11** 157
- Barj M, Lucazeau G and Delmas C 1992 *J. Solid State Chem.* **100** 141
- Brik Y, Kacimi M, Bozon-Verduraz F and Ziyad M 2001 *Micropor. Mesopor. Mater.* **43** 103
- Cushing Brian L and Goodenough J B 2001 *J. Solid State Chem.* **162** 176
- Elliott S R 1994 *Solid State Ionics* **70/71** 27
- Enrique Losilla R, Miguel A, Aranda G, Sebastian Bruque, Miguel A Paris, Jesus Sanz and West A R 1998 *Chem. Mater.* **10** 665
- Goodenough J B, Hong H Y P and Kafalas J A 1976 *Mater. Res. Bull.* **11** 203
- Gopalakrishnan J and Kasturi Rangan K 1992 *Chem. Mater.* **4** 745

- Govindan Kutty K V, Asuvathraman R and Sridharan R 1998 *J. Mater. Sci.* **33** 4007
- Hirose N and Kuwano J 1994 *J. Mater. Chem.* **4** 9
- Hong H Y P 1976 *Mater. Res. Bull.* **11** 173
- Irvine J T S and West A R 1989 in *High conductivity solid ionic conductors* (ed.) T Takahashi (Singapore: World Scientific) p. 201
- Jonscher A K 1980 *Phys. Thin Films* **11** 232
- Koteswara Rao K, Rambabu G, Raghavender M, Prasad G, Kumar G S and Vithal M 2005 *Solid State Ionics* **176** 2701
- Lightfoot P, Woodcock D A, Jorgensen J D and Short S 1999 *Int. J. Inorg. Mater.* **1** 53
- Lin Z, Yu H, Li S and Tian S 1988 *Solid State Ionics* **31** 91
- Masquelier C, Padhi A K, Nanjundaswamy K S and Goodenough J B 1998 *J. Solid State Chem.* **135** 228
- Mbandza A, Bordes E and Courtine P 1985 *Mater. Res. Bull.* **20** 251
- Meunier M *et al* 1998 *Appl. Surf. Sci.* **127** 466
- Nagganovsky Y K and Sigaryov S E 1992 *Solid State Ionics* **50** 1
- Nakamoto K 1978 *Infrared and Raman spectra of inorganic and coordination compounds* (New York: Wiley)
- Pasciak G, Prociow K, Mielcarek W, Gornicka B and Mazurek B 2001 *J. Euro. Ceram. Soc.* **21** 1867
- Rambabu G, Anantharamulu N, Vithal M, Raghavender M and Prasad G 2006 *J. Appl. Phys.* **100** 083707
- Rangan K K and Gopalakrishnan J 1995 *Inorg. Chem.* **34** 1969
- Rivier S, Angenault J and Couturier J C 1995 *Acta Crystallogr.* **C51** 1735
- Roy R, Vance E R and Alamo J 1982 *Mater. Res. Bull.* **17** 585
- Subramanian M A, Subramanian R and Clearfield A 1986 *Solid State Ionics* **18/19** 562
- Wang L and Kumar R V 2003 *Solid State Ionics* **158** 309
- Wu E 1989 *J. Appl. Crystallogr.* **22** 506